*Victor Iliev Rizov*

# DELAMINATION IN MULTI-LAYERED FUNCTIONALLY GRADED BEAMS – AN ANALYTICAL STUDY BY USING THE RAMBERG-OSGOOD EQUATION

# RASLOJAVANJE KOD VIŠESLOJNIH FUNKCIONALNIH KOMPOZITNIH NOSAČA – ANALITIČKA STUDIJA SA PRIMENOM RELACIJE RAMBERG-OSGOOD

Originalni naučni rad / Original scientific paper
UDK /UDC: 66.018.9:539.218
Rad primljen / Paper received: 20.01.2018

Adresa autora / Author's address:
University of Architecture, Civil Engineering and Geodesy, Department of Technical Mechanics, Sofia, Bulgaria,
email: v_rizov_fhe@uacg.bg

**Keywords**
- multi-layered beam
- functionally graded material
- delamination
- material nonlinearity
- analytical approach

*Abstract*

*The paper is focused on analysing the delamination fracture in multi-layered functionally graded cantilever beam structures which exhibit nonlinear mechanical behaviour of the material by using the Ramberg-Osgood equation. It is assumed that in each layer of the material is functionally graded in both thickness and length directions. The beam under consideration is made of adhesively bonded horizontal layers which have different thicknesses and material properties. The number of layers is arbitrary. Besides, the delamination crack is located arbitrary between layers. Power laws are applied to describe the continuous variation of the modulus of elasticity in each layer. A nonlinear solution for the strain energy release rate is derived by analysing the energy balance. The solution is verified by obtaining the strain energy release rate also by considering the complementary strain energy. Effects of the material gradients in thickness and length directions, the crack location along the beam height, the material nonlinearity and the crack length on the delamination fracture behaviour are elucidated.*

**Ključne reči**
- višeslojni nosač
- funkcionalni kompozitni materijal
- raslojavanje
- nelinearnost materijala
- analitički pristup

*Izvod*

*Rad je fokusiran na analizi loma raslojavanjem kod konstrukcije od višeslojnog nosača - konzole od funkcionalnog kompozitnog materijala, koja pokazuje nelinearno mehaničko ponašanje materijala, primenom relacije Ramberg-Osgood. Pretpostavlja se da je svaki sloj materijala funkcionalni kompozit u pravcu debljine i u pravcu dužine. Razmatrani nosač je izrađen od lepljenih horizontalnih slojeva koji imaju različite debljine i osobine materijala. Broj slojeva je proizvoljan. Prslina raslojavanja je proizvoljno locirana između slojeva. Jednačine sa stepenom funkcijom su primenjene za opisivanje kontinualne promene modula elastičnosti u svakom sloju. Nelinearno rešenje za brzinu oslobađanja energije deformacije je dobijeno analizom balansa energije. Rešenje je takođe provereno dobijanjem brzine oslobađanja energije razmatranjem komplementarne energije deformacije. Razjašnjeni su uticaji osobina materijala u smislu gradijenata po debljini i dužini, lokaciji prsline duž visine nosača, nelinearnosti materijala i od dužine prsline na ponašanje loma raslojavanjem.*

## INTRODUCTION

The application of functionally graded materials for manufacturing of various structural members, components and devices in aeronautics, nuclear reactors, electronics, optics, robotics and medicine has been constantly increasing for the last three decades, /1-8/. One of the main advantages of functionally graded materials over traditional structural materials is the fact that by continuously changing the microstructure of these new nonhomogeneous materials in one or more spatial directions during manufacture, their material properties can be tailored so as to attain optimum performance to the external loadings and influences. The study of fracture behaviour of functionally graded materials is very important for the safety design of functionally graded structures and components. However, due to the variation of the material properties, the fracture analysis of functionally graded materials and structures is more complicated in comparison to that of homogeneous materials.

Multi-layered functionally graded materials of adhesively bonded layers of different materials are used mainly in engineering applications where low weight is an important issue. The integrity, reliability and proper functioning of structures and components made of layered materials depend highly upon their delamination fracture behaviour /9, 10/. Up to now, delamination fracture in multi-layered functionally graded beams such as the crack lap shear and the split cantilever beam configurations which exhibit nonlinear mechanical behaviour of the material has been analysed mostly assuming that the material is functionally graded in the thickness direction of the layers, /11-13/. Usually, the nonlinear mechanical behaviour of the material is described by applying a power law stress-strain relation, /11-13/.

Therefore, the aim of the present paper is to analyse the delamination fracture in a multi-layered beam made of layers which are functionally graded in both thickness and length directions. Besides, it is assumed that in each layer the functionally graded material exhibits nonlinear mechanical behaviour that is described by the Ramberg-Osgood stress-strain relation. A solution for the strain energy release rate is derived by analysing the energy balance. It should be mentioned that the delamination fracture analysis performed in the present paper holds for nonlinear elastic behaviour of the material. The analysis can also be applied for elastic-plastic behaviour if the beam structure under consideration undergoes active deformation, i.e. if the external loading increases only /14, 15/. Also, the present analysis is developed assuming validity of the hypothesis for small strains.

## MATHEMATICAL FORMULATION

The present paper analyses the delamination fracture in the multi-layered functionally graded cantilever beam configuration shown in Fig. 1. The beam is made of adhesively bonded longitudinal horizontal layers. The number of layers is arbitrary. The layers have different thicknesses and material properties. It is assumed that in each layer the material is two-dimensional functionally graded (the elasticity modulus varies continuously in both thickness and in length direction). Besides, the material in each layer exhibits nonlinear mechanical behaviour. It is assumed that a delamination crack of length, $a$, is located arbitrarily between layers. Thus, the two crack arms have different thicknesses. The external loading consists of one vertical force, $F$, applied at the free end of the lower crack arm. Thus, the upper crack arm is free of stresses. The beam is clamped in its right-hand end. The cross-section of the beam is a rectangle of width, $b$, and height, $2h$. The beam length is denoted by $l$. The thicknesses of the lower and upper crack arms are denoted by $h_1$ and $h_2$, respectively.

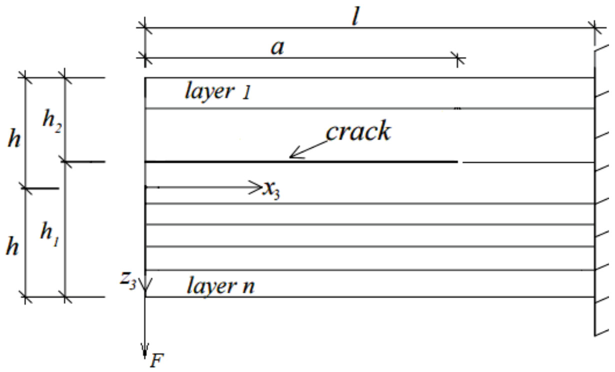


Figure 1. Multi-layered functionally graded cantilever beam with a delamination crack.

The delamination fracture is studied in terms of strain energy release rate, $G$, which is derived by analysing the energy balance. In order to derive $G$, an increase, $\delta a$, of the delamination crack length is assumed. The energy balance is written as

$$F\delta w_1 = \frac{\partial U}{\partial a}\delta a + Gb\delta a \,, \tag{1}$$

where: $w_1$ is the vertical displacement of the free end of the lower crack arm; $U$ is the strain energy cumulated in the beam. From Eq.(1), the strain energy release rate is obtained as

$$G = \frac{F}{b}\frac{\partial w_1}{\partial a} - \frac{1}{b}\frac{\partial U}{\partial a} \,. \tag{2}$$

The vertical displacement of the free end of the lower crack arm is written as

$$w_1 = \int_0^a x_3\kappa_1 dx_3 + \int_a^l x_3\kappa_2 dx_3 \,, \tag{3}$$

where: $\kappa_1$ and $\kappa_2$ are, respectively, the curvatures of the lower crack arm and the uncracked beam portion, $a \le x_3 \le l$. The longitudinal axis, $x_3$, is shown in Fig. 1.

The curvature of the lower crack arm is determined from the following equations for equilibrium of the cross-section of the lower crack arm:

$$N_1 = b\sum_{i=1}^{i=n_L}\int_{z_{1i}}^{z_{1i+1}} \sigma_i dz_1 \,, \tag{4}$$

$$M_{y_1} = b\sum_{i=1}^{i=n_L}\int_{z_{1i}}^{z_{1i+1}} \sigma_i z_1 dz_1 \,, \tag{5}$$

where: $n_L$ is the number of layers in the lower crack arm; $z_{1i}$ and $z_{1i+1}$ are, respectively, the coordinates of the upper and lower surfaces of the $i$-th layer; $\sigma_i$ is the distribution of longitudinal normal stresses in the same layer; $z_1$ is the vertical centroidal axis (Fig. 2); $N_1$ and $M_{y1}$ are, respectively, the longitudinal force and bending moment in the lower crack arm. It is obvious that (see Fig. 1)

$$N_1 = 0 \,, \tag{6}$$

$$M_{y_1} = Fx_3 \,. \tag{7}$$

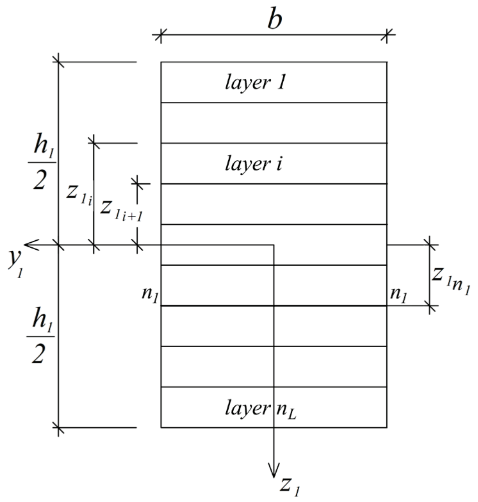


Figure 2. Geometry of the cross-section of the lower crack arm.

The mechanical behaviour of the functionally graded material in the $i$-th layer is described by the Ramberg-Osgood stress-strain relation

$$\varepsilon = \frac{\sigma_i}{E_i} + \left(\frac{\sigma_i}{H_i}\right)^{\frac{1}{m_i}} \,, \tag{8}$$

where: $\varepsilon$ is the distribution of the longitudinal strains in the cross-section; $E_i$ is the modulus of elasticity; $H_i$ and $m_i$ are material properties in the same layer.

It is assumed that the modulus of elasticity is distributed continuously in the thickness direction of the $i$-th layer according to the following power law:

$$E_i = E_{g_i} + \frac{E_{d_i} - E_{g_i}}{(z_{1i+1} - z_{1i})^{q_i}} (z_1 - z_{1i})^{q_i}, \quad (9)$$

where:

$$z_{1i} \le z_1 \le z_{1i+1}. \quad (10)$$

In Eq.(9), $E_{gi}$ and $E_{di}$ are, respectively, the values of the modulus of elasticity in the upper and lower surfaces of the $i$-th layer; $q_i$ is a material property. The following power laws are applied to describe the continuous variation of $E_{gi}$ and $E_{di}$ along the beam length:

$$E_{g_i} = E_{g_i}^f + \frac{E_{g_i}^r - E_{g_i}^f}{l^{s_i}} x_3^{s_i}, \quad (11)$$

$$E_{d_i} = E_{d_i}^f + \frac{E_{d_i}^r - E_{d_i}^f}{l^{s_i}} x_3^{s_i}, \quad (12)$$

where:

$$0 \le x_3 \le l. \quad (13)$$

In Eqs.(11) and (12), $E_{gi}{}^f$ and $E_{di}{}^f$ are the values, in respect, of $E_{gi}$ and $E_{di}$ in the beam free end. The values of $E_{gi}$ and $E_{di}$ in the clamped end of the beam are denoted by $E_{gi}{}^r$ and $E_{di}{}^r$, respectively. It can be recapitulated that Eqs.(9), (11) and (12) describe the distribution of the modulus of elasticity in the thickness and length directions in $i$-th layer of the beam.

In the present paper, the distribution of the longitudinal strains along the height of the cross-section is analysed assuming validity of the Bernoulli's hypothesis for plane sections since the span-to-height ratio of the beam under consideration is large. Thus, the distribution of $\varepsilon$ is written as

$$\varepsilon = \kappa_1 (z_1 - z_{1n_1}), \quad (14)$$

where: $z_{1n1}$ is the coordinate of the neutral axis (Fig. 2). It should be noted that the neutral axis, $n_1n_1$, shifts from the centroid since the beam is multi-layered and functionally graded.

In order to perform the integration in Eqs.(4) and (5), $\sigma_i$ has to be expressed as a function of $z_1$. However, it is obvious that $\sigma_i$ cannot be determined explicitly from Eq.(8). Therefore, $\sigma_i$ is expanded in series of Maclaurin by keeping the first three members

$$\sigma_i(z_1) = \sigma_i(0) + \frac{\sigma_i'(0)}{1!} z_1 + \frac{\sigma_i''(0)}{2!} z_1^2. \quad (15)$$

Equation (15) is rewritten as

$$\sigma_i(z_1) = \delta_i + \varphi_i z_1 + \eta_i z_1^2, \quad (16)$$

where: coefficients, $\delta_i$, $\phi_i$ and $\eta_i$, are determined in the following manner. First, by substituting Eqs.(9), (14) and (16) into Eq.(8), one obtains

$$H_i^{\frac{1}{m_i}} (\kappa_1 z_1 - \kappa_1 z_{1n_1}) \left[ E_{g_i} + \beta_i (z_1 - z_{1i})^{q_i} \right] = H_i^{\frac{1}{m_i}} (\delta_i + \varphi_i z_1 + \eta_i z_1^2) + \left[ E_{g_i} + \beta_i (z_1 - z_{1i})^{q_i} \right] (\delta_i + \varphi_i z_1 + \eta_i z_1^2)^{\frac{1}{m_i}}, \quad (17)$$

where:

$$\beta_i = \frac{E_{d_i} - E_{g_i}}{(z_{1i+1} - z_{1i})^{q_i}}. \quad (18)$$

By substituting $z_1 = 0$ in Eq.(14), one arrives at

$$-H_i^{\frac{1}{m_i}} \kappa_1 z_{1n_1} \left[ E_{g_i} + \beta_i (-z_{1i})^{q_i} \right] = H_i^{\frac{1}{m_i}} \delta_i + \left[ E_{g_i} + \beta_i (-z_{1i})^{q_i} \right] \delta_i^{\frac{1}{m_i}}. \quad (19)$$

By differentiating Eq.(17) with respect to $z_1$ and then substituting $z_1 = 0$, one derives

$$H_i^{\frac{1}{m_i}} \kappa_1 \left[ E_{g_i} + \beta_i (-z_{1i})^{q_i} \right] - H_i^{\frac{1}{m_i}} \kappa_1 z_{1n_1} q_i \beta_i (-z_{1i})^{q_i - 1} = H_i^{\frac{1}{m_i}} \varphi_i + q_i \beta_i (-z_{1n_1})^{q_i - 1} \delta_i^{\frac{1}{m_i}} + \left[ E_{g_i} + \beta_i (-z_{1i})^{q_i} \right] \frac{1}{m_i} \delta_i^{\frac{1-m_i}{m_1}} \varphi_i. \quad (20)$$

By substituting $z_1 = 0$ in the second derivative of Eq.(17) with respect to $z_1$, one obtains

$$H_i^{\frac{1}{m_i}} \kappa_1 \beta_i q_i (-z_{1n_1})^{q_i - 1} + H_i^{\frac{1}{m_i}} \kappa_1 q_i \beta_i (-z_{1i})^{q_i - 1} - H_i^{\frac{1}{m_i}} \kappa_1 z_{1n_1} q_i \beta_i (q_i - 1)(-z_{1i})^{q_i - 2} = 2 H_i^{\frac{1}{m_i}} \eta_i + q_i \beta_i (q_i - 1)(-z_{1n_1})^{q_i - 2} \delta_i^{\frac{1}{m_i}} +$$
$$+ q_i \beta_i (-z_{1n_1})^{q_i - 1} \frac{1}{m_i} \delta_i^{\frac{1-m_i}{m_i}} \varphi_i + \left[ E_{g_i} + \beta_i (-z_{1i})^{q_i} \right] \frac{1}{m_i} \left( \frac{1-m_i}{m_i} \delta_i^{\frac{1-2m_i}{m_i}} \varphi_i^2 + 2 \delta_i^{\frac{1-m_i}{m_i}} \eta_i \right) \quad (21)$$

It should be noted that Eqs.(19), (20) and (21) can be written for each layer in the lower crack arm. Thus, the number of equations is $3n_L$. In these equations, there are $2 + 3n_L$ unknowns, $\kappa_1$, $z_{1n1}$, $\delta_i$, $\phi_i$ and $\eta_i$, where $i = 1, 2, \dots n_L$. Two more equations are obtained by substituting Eq.(16) into Eqs.(4) and (5):

$$N_1 = b\sum_{i=1}^{i=n_1}\left[\delta_i(z_{1i+1}-z_{1i})+\frac{1}{2}\varphi_i(z_{1i+1}^2-z_{1i}^2)+\frac{1}{3}\eta_i(z_{1i+1}^3-z_{1i}^3)\right], \tag{22}$$

$$M_{y_1} = b\sum_{i=1}^{i=n_1}\left[\frac{1}{2}\delta_i(z_{1i+1}^2-z_{1i}^2)+\frac{1}{3}\varphi_i(z_{1i+1}^3-z_{1i}^3)+\frac{1}{4}\eta_i(z_{1i+1}^4-z_{1i}^4)\right]. \tag{23}$$

In this way, one obtains $2 + 3n_L$ equations which should be solved with respect to $\kappa_1$, $z_{1n1}$, $\delta_i$, $\phi_i$ and $\eta_i$, where $i = 1, 2, \dots n_L$, by using the MatLab computer program. It should also be noted that these equations can be applied to determine $\kappa_1$, $z_{1n1}$, $\delta_i$, $\phi_i$ and $\eta_i$, where $i = 1, 2, \dots n_L$, in any cross-section of the lower crack arm, i.e. at any abscise, $x_3$, in the interval $[0; a]$.

The same equations can also be used to determine $\kappa_2$, $z_{2n2}$, $\delta_{Bi}$, $\phi_{Bi}$ and $\eta_{Bi}$, where $i = 1, 2, \dots n$, (here, $\kappa_2$ and $z_{2n2}$ are, respectively, the curvature and the coordinate of the neutral axis of the cross-section of the uncracked beam portion, $\delta_{Bi}$, $\phi_{Bi}$ and $\eta_{Bi}$ are the parameters of the stress state of the $i$-th layer, $n$ is the number of layers in the uncracked beam portion). For this purpose, $n_L$, $\kappa_1$, $z_{1i}$, $z_{1i+1}$, $z_{1n1}$, $\delta_i$, $\phi_i$, and $\eta_i$ have to be replaced with $n$, $\kappa_2$, $z_{2i}$, $z_{2i+1}$, $z_{2n2}$, $\delta_{Bi}$, $\phi_{Bi}$, and $\eta_{Bi}$, respectively (here, $z_{2i}$ and $z_{2i+1}$ are the coordinates, respectively, of the upper and lower surfaces of the $i$-th layer).

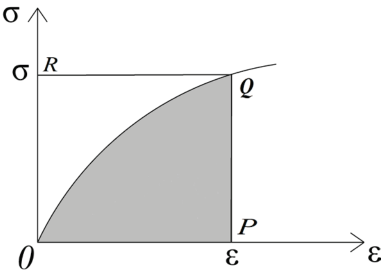


Figure 3. Nonlinear stress-strain curve.

The strain energy cumulated in the beam is written as

$$U = U_A + U_B, \tag{24}$$

where: $U_A$ and $U_B$ are the strain energies in the lower crack arm and the uncracked beam portion, respectively.

The strain energy in the lower crack arm is obtained by addition of the strain energies in the layers

$$U_A = b\sum_{i=1}^{i=n_L}\int_0^a\int_{z_{1i}}^{z_{1i+1}} u_{0A_i}\,dx_3 dz_1, \tag{25}$$

where: $u_{0Ai}$ is the strain energy density in the $i$-th layer. In principle, the strain energy density is equal to the area, OPQ, enclosed by the stress-strain curve (Fig. 3). For the Ramberg-Osgood stress-strain relation, the strain energy density can be calculated by the following formula, /16/:

$$u_{0A_i} = \frac{\sigma_i^2}{2E_i}+\frac{\sigma_i^{\frac{1+m_i}{m_i}}}{(1+m_i)H^{\frac{1}{m_i}}}, \tag{26}$$

where: $E_i$ and $\sigma_i$ are obtained by Eqs.(9) and (16), in respect.

The strain energy in the uncracked beam portion is written as

$$U_B = b\sum_{i=1}^{i=n}\int_a^l\int_{z_{2i}}^{z_{2i+1}} u_{0B_i}\,dx_3 dz_2, \tag{27}$$

where: the strain energy density, $u_{0Bi}$, is found by Eq.(26). For this purpose, $\sigma_i$ is determined by replacing $\delta_i$, $\phi_i$ and $\eta_i$, respectively, with $\delta_{Bi}$, $\phi_{Bi}$ and $\eta_{Bi}$ in Eq.(16).

Finally, by substituting Eqs.(3), (24), (25) and (27) into Eq.(2) one arrives at

$$G = \frac{F}{b}a\left[\kappa_1(a)-\kappa_2(a)\right]-\sum_{i=1}^{i=n_L}\int_{z_{1i}}^{z_{1i+1}} u_{0A_i}(a)dz_1 + \sum_{i=1}^{i=n}\int_{z_{2i}}^{z_{2i+1}} u_{0B_i}(a)dz_2 \tag{28}$$

where: $\kappa_1(a)$, $\kappa_2(a)$, $u_{0Ai}(a)$ and $u_{0Bi}(a)$ are obtained by Eqs.(19), (20), (21), (2) and (23) at $x_3 = a$. The integration in Eq.(28) should be performed by the MatLab computer programme.

In order to verify Eq.(28), the strain energy release rate is determined also by applying the following formula, /11/:

$$G = \frac{dU^*}{bda}, \tag{29}$$

where: $dU^*$ is the change in the complementary strain energy; $da$ is an elementary increase of delamination crack length.

The complementary strain energy cumulated in the beam is written as

$$U^* = U_A^* + U_B^*, \tag{30}$$

where: $U_A^*$ and $U_B^*$ are the complementary strain energies in the lower crack arm and the uncracked beam portion, in respect.

The complementary strain energy in the lower crack arm is expressed as

$$U_A^* = b\sum_{i=1}^{i=n_L}\int_0^a\int_{z_{1i}}^{z_{1i+1}} u_{0A_i}^*\,dx_3 dz_1, \tag{31}$$

where: $u^*_{0Ai}$ is the complementary strain energy density in the $i$-th layer. The complimentary strain energy density is equal to the area OQR that supplements the area OPQ to a rectangle (Fig. 3). Thus, $u^*_{0Ai}$ is written as

$$u_{0A_i}^* = \sigma_i\varepsilon - u_{0A_i}. \tag{32}$$

By combining Eqs.(8), (9), (26) and (32), one derives

$$u_{0A_i}^* = \frac{\sigma_i^2}{2\left[E_{g_i}+\beta_i(z_1-z_{1i})^{q_i}\right]}+\frac{m_i\sigma_i^{\frac{1+m_i}{m_i}}}{(1+m_i)H^{\frac{1}{m_i}}}, \tag{33}$$

where: $\sigma_i$ is found by Eq.(16).

The complementary strain energy in the uncracked beam portion is obtained as

$$U_B^* = b\sum_{i=1}^{i=n}\int_a^l\int_{z_{2i}}^{z_{2i+1}} u_{0B_i}^* dx_3 dz_2 \,, \tag{34}$$

where: the complementary strain energy density, $u^*_{0Bi}$, in the $i$-th layer is found by Eq.(33). For this purpose, $z_1$ and $z_{1n1}$ are replaced with $z_2$ and $z_{2n2}$, respectively. Besides, $\sigma_i$ is calculated by Eq.(16) by replacing $\delta_i$, $\phi_i$, and $\eta_i$ with $\delta_{Bi}$, $\phi_{Bi}$ and $\eta_{Bi}$, respectively.

By substituting Eqs.(30), (31) and (34) into Eq.(29), one arrives at

$$G = \sum_{i=1}^{i=n_L}\int_{z_{1i}}^{z_{1i+1}} u_{0A_i}^*(a)dz_1 - \sum_{i=1}^{i=n}\int_{z_{2i}}^{z_{2i+1}} u_{0B_i}^*(a)dz_2 \,, \tag{35}$$

where: $u^*_{0Ai}(a)$ and $u^*_{0Bi}(a)$ are determined by Eq.(33) at $x_3 = a$. The integration in Eq.(35) should be carried out by using the MatLab computer programme. The strain energy release rate obtained by Eq.(35) is exact match of the strain energy release rate found by Eq.(28). This fact is a verification of the nonlinear delamination fracture analysis of the multi-layered two-dimensional functionally graded cantilever beam, developed in the present paper.

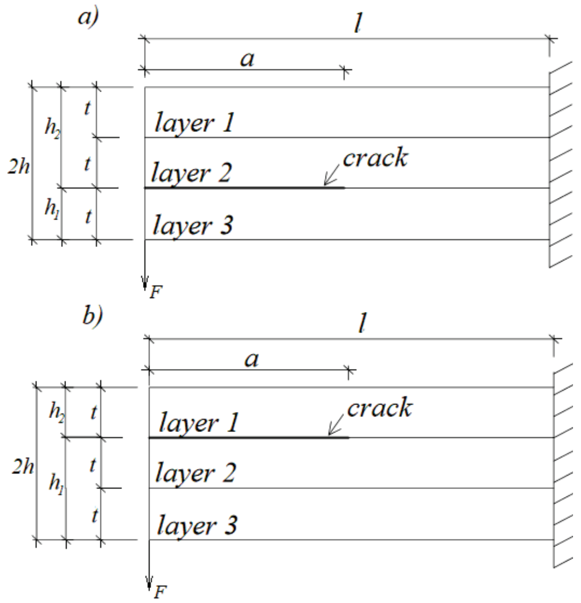


Figure 4. Two three-layered functionally graded cantilever beam configurations containing a delamination crack between: ($a$) layers 2 and 3; and ($b$) layers 1 and 2.

It should be noted that the delamination fracture is analysed also by keeping more than three members in the series of Maclaurin, Eq.(15). The results obtained are very close to these obtained by keeping the first three members (the difference is less than 3 %).

## PARAMETRIC INVESTIGATIONS

Parametric investigations are performed in order to elucidate the effects of the material gradients in the thickness and length directions, the crack location along the height of the beam cross-section and the nonlinear mechanical behaviour of the functionally graded material on the delamination fracture. For this purpose, calculations of the strain energy release rate are carried out by applying Eq.(28).

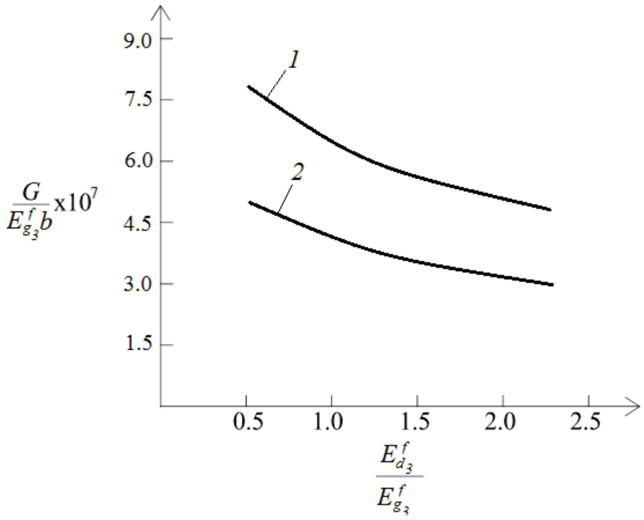


Figure 5. The strain energy release rate in non-dimensional form presented as a function of $E_{d_3}^f / E_{g_3}^f$ ratio (curve 1 - for delamination crack located between layers 2 and 3 (refer to Fig. 4a); curve 2 - for delamination crack located between layers 1 and 2 (refer to Fig. 4b)).

The results obtained are presented in non-dimensional form by using the formula $G_N = G/(E_{g_3}^f b)$. In order to elucidate the influence of the crack location along the beam height on the delamination fracture behaviour, two three-layered functionally graded cantilever beam configurations are analysed (Fig. 4). A delamination crack is located between layers 2 and 3 in the beam shown in Fig. 4a. A beam containing a delamination crack between layers 1 and 2 is also investigated (Fig. 4b). In both beam configurations, the thickness of layers is $t$ (Fig. 4). It is assumed that $F = 40$ N, $b = 0.015$ m, $t = 0.003$ m and $l = 0.25$ m. The material gradient in the thickness direction of layer 3 is characterized by $E_{d_3}^f / E_{g_3}^f$ ratio. The strain energy release rate in non-dimensional form is presented as a function of $E_{d_3}^f / E_{g_3}^f$ ratio in Fig. 5 for the two beam configurations (Fig. 4) assuming that $E_{g_2}^f / E_{g_3}^f = 0.7$, $E_{d_2}^f / E_{g_2}^f = 0.9$, $E_{g_1}^f / E_{g_3}^f = 0.5$, $E_{d_1}^f / E_{g_1}^f = 0.6$, $E_{g_3}^r / E_{g_3}^f = 0.5$, $E_{d_3}^r / E_{g_3}^r = 0.9$, $E_{g_2}^r / E_{g_3}^r = 0.7$, $E_{d_2}^r / E_{g_2}^r = 0.6$, $E_{g_1}^r / E_{g_3}^r = 0.8$, $E_{d_1}^r / E_{g_1}^r = 0.9$, $s_1 = s_2 = s_3 = 0.6$, $q_1 = q_2 = q_3 = 0.4$, $H_3 / E_{g_3}^f = 0.5$, $H_2 / H_3 = 0.7$, $H_1 / H_3 = 0.6$, $m_1 = m_2 = m_3 = 0.8$ and $a/l = 0.7$. One can observe in Fig. 5 that the strain energy release rate decreases with the increase of the $E_{d_3}^f / E_{g_3}^f$ ratio. This behaviour is due to the increase of the beam stiffness. It can also be observed that the strain energy release rate is higher when the delamination crack is located between layers 2 and 3. This finding is attributed to the fact that the stiffness of the lower crack arm is lower when the delamination crack is between layers 2 and 3.

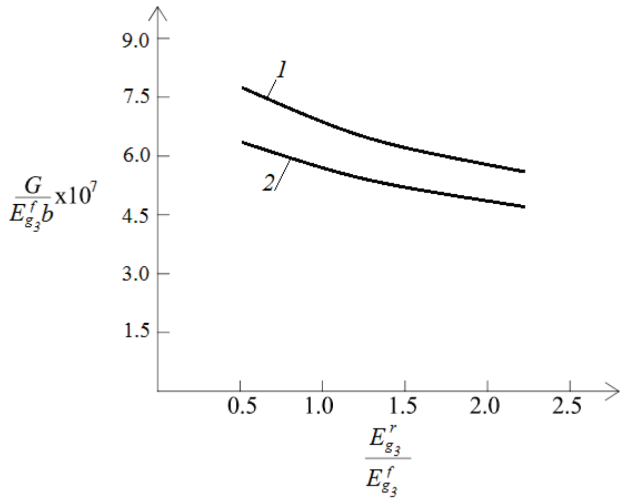


Figure 6. The strain energy release rate in non-dimensional form presented as a function of $E^r_{g_3} / E^f_{g_3}$ ratio (curve 1 - at nonlinear behaviour of the functionally graded material, curve 2 - at linear-elastic behaviour of the functionally graded material).

The $E^r_{g_3} / E^f_{g_3}$ ratio characterizes the material gradient along the beam length in layer 3. In order to evaluate the influence of $E^r_{g_3} / E^f_{g_3}$ ratio on the delamination fracture behaviour, the strain energy release rate in non-dimensional form is plotted against $E^r_{g_3} / E^f_{g_3}$ ratio in Fig. 6 for the three-layered functionally graded beam configuration containing a delamination crack between layers 2 and 3 (refer to Fig. 4a). It can be observed in Fig. 6 that the strain energy release rate decreases with the increase of $E^r_{g_3} / E^f_{g_3}$ ratio. In order to elucidate the effect of the nonlinear mechanical behaviour of the functionally graded material on the delamination fracture, the strain energy release rate in non-dimensional form is plotted against $E^r_{g_3} / E^f_{g_3}$ ratio in Fig. 6, also assuming linear-elastic behaviour of the functionally graded material (the linear-elastic solution for the strain energy release rate is obtained by substituting $H_i \to \infty$, where $i = 1, 2, \ldots 3$, in Eqs.(19), (20), (21), (26) and (28), which follows from the fact that at $H_i \to \infty$ the Ramberg-Osgood stress-strain relation, Eq.(8), transforms into Hooke's law. The curves in Fig. 6 indicate that the nonlinear mechanical behaviour of the functionally graded material leads to the increase of strain energy release rate.

The effect of delamination crack length on nonlinear fracture behaviour is evaluated too (the delamination crack length is characterized by *a/l* ratio). For this purpose, the strain energy release rate in non-dimensional form is presented as a function of *a/l* ratio in Fig. 7 at various $H_3 / E^f_{g_3}$ ratios (the three-layered functionally graded cantilever beam configuration shown in Fig. 4a is analysed). One can observe in Fig. 7 that the strain energy release rate increases with the increase of *a/l* ratio (this is due from the increase of bending moment and from the decrease of the elasticity modulus in the beam cross-section, where the crack tip is located; the modulus of elasticity decreases with the increase of delamination crack length since $E^r_{g_3} / E^f_{g_3} = 0.5$). The diagrams in Fig. 7 indicate also that the strain energy release rate decreases with the increase of $H_3 / E^f_{g_3}$ ratio.

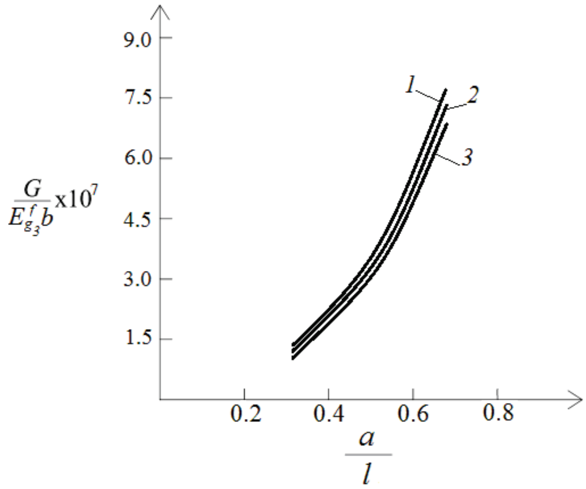


Figure 7. The strain energy release rate in non-dimensional form presented as a function of *a/l* ratio (curve 1 - at $H_3 / E^f_{g_3} = 0.5$, curve 2 - at $H_3 / E^f_{g_3} = 2$, curve 3 - at $H_3 / E^f_{g_3} = 8$).

## CONCLUSIONS

Delamination fracture in a multi-layered functionally graded cantilever beam is analysed assuming nonlinear mechanical behaviour of the material. The beam is made of an arbitrary number of adhesively bonded horizontal layers with different thicknesses and material properties. In each layer, the material is functionally graded in both thickness and length directions (i.e., the material is two-dimensional functionally graded). A delamination crack is located arbitrarily between layers. The beam is loaded by one vertical force applied at the free end of the lower crack arm. The nonlinear behaviour of the functionally graded material is described by the Ramberg-Osgood stress-strain relation. The continuous variation of the modulus of elasticity in thickness and length directions is described by power laws in each layer. The delamination fracture is studied in terms of the strain energy release rate by analysing the balance of energy. The strain energy release rate is derived also by considering the complementary strain energy for verification. Effects of the material gradients in thickness and length directions, the nonlinear mechanical behaviour of the functionally graded material, the crack location along the height of the beam cross-section and the crack length vs. the delamination fracture are elucidated. Analysis reveals that the strain energy release rate decreases with increasing of $E^f_{d_3} / E^f_{g_3}$, $E^r_{g_3} / E^f_{g_3}$ and $H_3 / E^f_{g_3}$ ratios. It is found also that the strain energy release rate decreases when the thickness of the lower crack arm increases. The results obtained indicate that the strain energy release rate increases with an increase of crack length, when $E^r_{g_3} / E^f_{g_3} = 0.5$. The analysis developed in the present paper shows that the delamination fracture in multi-layered functionally graded cantilever beams which exhibit nonlinear mechanical behaviour of the material can be controlled by using appropriate material gradients in both thickness and length directions.

REFERENCES


1. Neubrand, A., Rödel, J. (1997), *Gradient materials: An overview of a novel concept,* Zeit. f. Met. 88(1):358-371.
2. Suresh, S., Mortensen, A., Fundamentals of Functionally Graded Materials: Processing and Thermomechanical Behavior of Graded Metals and Metal-Ceramic Composites, IOM Communications Ltd, London, 1998.
3. Hirai, T., Chen, L. (1999), *Recent and prospective development of functionally graded materials in Japan*, Mater Sci. Forum, 308-311(2):509-514.
4. Gasik, M.M. (2010), *Functionally graded materials: bulk processing techniques,* Int. J Mater. Prod. Tech. 39(1-2):20-29. doi.org/10.1504/IJMPT.2010.034257
5. Tokova, L., Yasinskyy, A., Ma, C.-C. (2017), *Effect of the layer inhomogeneity on the distribution of stresses and displacements in an elastic multilayer cylinder*, Acta Mechanica, 228(8):2865-2877 doi: 10.1007/s00707-015-1519-8
6. Tokovyy, Y., Ma, C.-C. (2016), *Axisymmetric stresses in an elastic radially inhomogeneous cylinder under length-varying loadings*, ASME J Appl. Mech., 83(11): 111007 doi: 10.1115/1.4034459.
7. Uslu Uysal, M. (2016), *Buckling behaviours of functionally graded polymeric thin-walled hemispherical shells*, Steel and Comp. Struc., 21(4):849-862. doi: 10.12989/scs.2016.21.4.849
8. Uslu Uysal, M., Güven, U. (2016), *A bonded plate having orthotropic inclusion in adhesive layer under in-plane shear loading*, The J Adhesion, 92(3): 214-235. doi: 10.1080/00218464.2015.1019064.
9. Dolgov, N.A. (2005), *Determination of stresses in a two-layer coating,* Strength of Mater., 37(4):422-431. doi.org/10.1007/s11223-005-0053-7
10. Dolgov, N.A. (2016), *Analytical methods to determine the stress state in the substrate-coating system under mechanical loads*, Strength of Mater., 48(5):658-667. doi: 10.1007/s11223-016-9809-5
11. Rizov, V.I. (2017), *Delamination fracture in a functionally graded multilayered beam with material nonlinearity*, Archive of Appl. Mech., 87(6):1037-1048. doi.org/10.1007/s00419-017-1229-x
12. Rizov, V.I. (2017), *Non-linear elastic delamination of multi-layered functionally graded beam*, Multidisc. Model. in Mater. and Struc., 13(3):434-447. doi: 10.1108/MMMS-10-2016-0054
13. Rizov, V.I. (2018), *Delamination of multilayered functionally graded beams with material nonlinearity*, Int. J Struc. Stability and Dyn., 18(4):1850051 doi.org/10.1142/S0219455418500517
14. Chakrabarty, J., Theory of Plasticity, 3rd Ed., Elsevier Butterworth-Heinemann, Oxford, 2006.
15. Lubliner, J., Plasticity Theory (Revised Edition), University of California, Berkeley, CA, 2006.
16. Rizov, V. (2017), *Delamination analysis of a layered elastic-plastic beam*, Int. J Struc. Integ., 8(5):516-529. doi.org/10.1108/IJSI-11-2016-0035